Common image gathers from blended data

Ziguang Su and Daniel Trad

ABSTRACT

Common-image gathers, or CIGs, are essential for migration-based velocity analysis and amplitude-versus-angle analysis, which could be utilized to predict lithology, fluid properties, and create velocity models. Blended acquisition, also known as simultaneous seismic source acquisition, is a useful technique for boosting acquisition efficiency and improving the quality of the subsurface image. We offer a technique that uses reverse time migration based on direction vectors to calculate angle-domain common-image gathers (ADCIGs) straight from blended data. Our technique generates amplitude-preserved ADCIGs and takes into account subsurface folds in the image condition. Examples that contrast our method with exact Zoeppritz equations demonstrate its correctness. Our strategy also allows for the loosing of the acquisition restrictions of random source timings and placements.

INTRODUCTION

Blended acquisiton

The blended acquisition technique targets at removing the limitation of no interference between adjacent shots by allowing sources to be shot simultaneously (Berkhout et al., 2009). While conventional acquisitions record energy coming from only one source at a time, blended acquisitions record energy coming from multiple sources simultaneously (Garottu, 1983; Beasley et al., 1998; Berkhout, 2008), as shown in Figure 1.

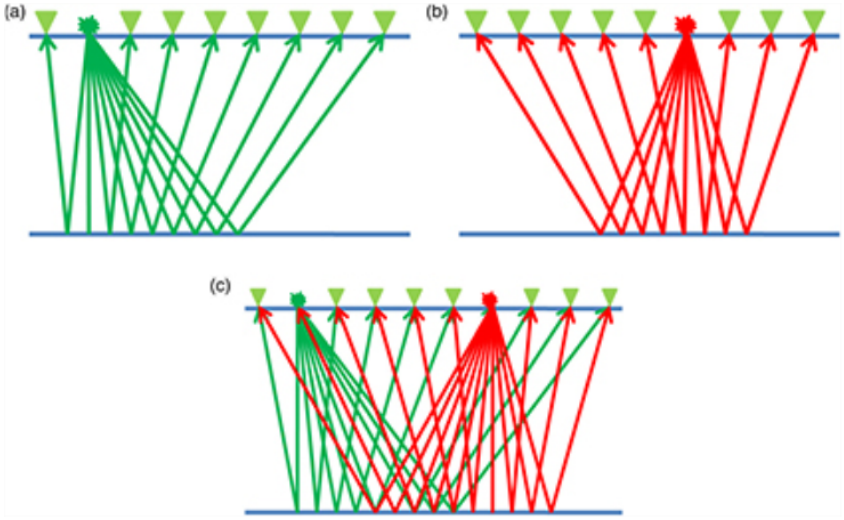

FIG. 1. (a) and (b) are illustrations of conventional single shot acquisition and (c) is blended shot acquisition.

When seismic sources are acquired simultaneously, data quality is improved (e.g., through

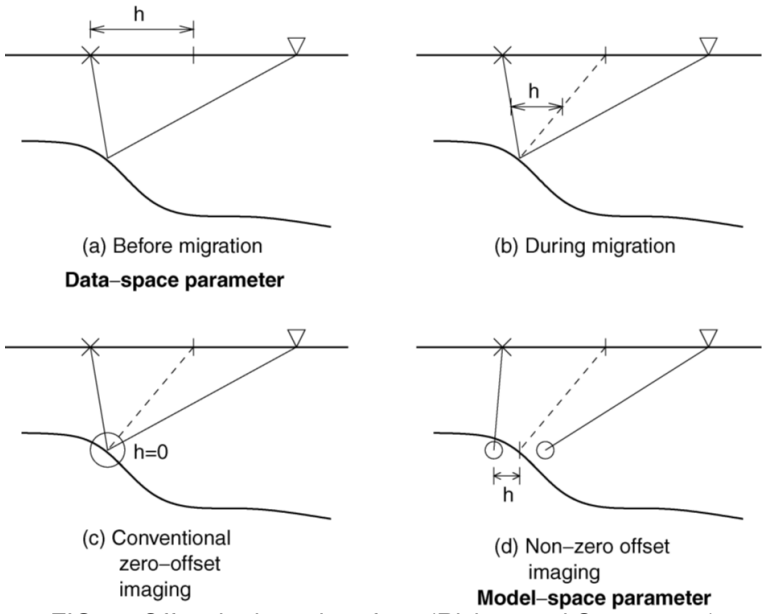

FIG. 2. Offset in the subsurface (Rickett and Sava, 2002)

denser shooting) and acquisition costs are reduced. This is possible because simultaneous seismic source acquisition permits temporal overlap between shot recordings (e.g., efficient wide-azimuth shooting).

Common image gather

A common image gather/CIG for a reflection point is a series of prestack migrated trace at the given image point (Jin et al., 2014). CIGs are the primary data for the techniques of amplitude variation with offset (AVO), or amplitude variation with incidence angle (AVA), which has been used to predict subsurface attribute interpretation for decades (Ostrander, 1984). CIGs can be extracted as a function of the subsurface attributes, such as subsurface offsets or reflection angles. CIGs taking offset are called offset-domain common-image gathers (ODCIGs).The offset in ODCIG normally refers to the distance between the shot and receiver on the surface. Later the concept of offset was extended to the subsurface offset between the upgoing and downgoing wavefields (Rickett and Sava, 2002), as shown in Fig 2. Offset changes from a data-space parameter to a model-space parameter by migration. In a reflection raytrace, the subsurface offset is continuous as the depth increases. The ODCIGs can be produced by either Kirchhoff migration or wavefield continuation migration (Sava and Fomel, 2003). However, ODCIGs fail to properly characterize commplex propagation path because of the ambiguity of reflector positions caused by multipathing(Nolan and Symes, 1996). ODCIGs also have problem calculating subsurface fold as we will discuss later.

The problems in ODCIGs can be alleviated by ADCIGs. Similar to ODCIGs, the ADCIGs can also be produced by pre-imaging methods like Kirchhoff methods (Xu et al., 2001) or wave-equation methods (De Bruin et al., 1990). These two methods are based on the wave equation, so there's no sensitivity to the ray-traced angle. The ADCIGs can also be computed after-imaging (Biondi and Shan, 2002; Rickett and Sava, 2002) or transferred from ODCIG by Fourier Transform (Sava and Fomel, 2003).

True amplitude RTM

RTM is a migration method that is based on the two-way wave equation. Compared with migration methods based on the one-way wave equation, RTM has better results for complex structures like salt structures. RTM is initially introduced by many authors (Baysal et al., 1983; Whitmore, 2005; McMECHAN, 1983).

To migrate a shot gather $Q(x, y; x_s, y_x; t)$ using conventional RTM, we need to compute wavefields shot at the source location and seismic traces recorded at the receiver location, with a source at $(x_s, y_s, z_s = 0)$ and receivers at $(x, y, z = 0)$. The two-way acoustic wave equation goes:

$$(\frac{1}{c^2}\frac{\partial^2}{\partial t^2}p_F(\overrightarrow{x};t) = \delta(\overrightarrow{x} - \overrightarrow{x_s})f(t) \tag{1}$$

and

$$\begin{cases}(\frac{1}{c^2}\frac{\partial^2}{\partial t^2} - \nabla^2)p_B(\overrightarrow{x};t) = 0\\ p_B(x, y.z = 0; t) = Q(x, y; x_s, y_x; t)\end{cases} \tag{2}$$

where p_F and p_B are forward wavefield and backward wavefield respectively, $c = c(x, y, z)$ is the velocity, $f(t)$ is the wavelet function, and ∇^2 is the Laplacian operator.

To get a common shot image with correct migration amplitude, we need to apply "deconvolution" image conditions(ICs)(Zhang et al., 2005):

$$R(\overrightarrow{x}) = \int p_B(\overrightarrow{x};t)p_F^{-1}(\overrightarrow{x};t)dt \tag{3}$$

METHOD

Hypotheses

1. The earth's response can generally be approximated as linear and any response to any complex force can be calculated as a sum of the displacement of constituent body forces. Similarly, the response to multiple seismic sources can be considered a sum of responses to each independent source.
2. There is only one wave direction per image point per image time. (Vyas et al., 2011)
3. The AVA response curve is continuous when the angle interval is relatively small.

Direct migration of blended data

The largest issue in simultaneous-source processing is intense crosstalk noise between adjacent shots, which poses a challenge for conventional processing (Chen et al., 2014). Simultaneous-acquired data/blended data can be processed by either directly inverting for model properties(Dai et al., 2011)(Tang and Biondi, 2009) or separating blended data into deblended data(Berkhout, 2008; Mahdad et al., 2011; Akerberg et al., 2008; Beasley, 2008; Abma and Yan, 2009), called "deblending" (Berkhout, 2008).

There are some issues with both direct migration and deblending/gather separation. Direct migration contaminates images by crosstalk and has a higher request for velocity model accuracy compared with deblending. Separating the blended gathers can be difficult when shot spacing is close and too many shots are blended. Deblending also can be very difficult for complex models containing many scatter points(Tang and Biondi, 2009). And successful methods of separating data rely strongly on random source timings and positions (Abma and Yan, 2009; Moore et al., 2008). Loosing these acquisition restrictions will make survey design and implementation more flexible (Leader and Biondi).

ADCIG extraction from RTM

There are many migration methods that can extract ADCIGs. Compared with the formulations of true amplitude Kirchhoff migration (Bleistein, 1987; Bleistein et al., 2001) and one-way wavefield migration (Zhang et al., 2005), true amplitude RTM is much simpler because the propagator itself naturally carries the correct propagation amplitude if the shot record is well approximated by solving the wave equation (Zhang and Sun, 2009). Because the RTM is based on the direct solutions of the wave equation, energy associated with multiple scatter events, steep drops and a broad range of wavenumbers will be preserved.

Methods for extracting angle-domain common-image gathers (ADCIGs) during 2D reverse-time migration fall into three main categories; direction-vector-based methods (DVB), local-plane-wave decomposition methods (LPWD), and local-shift imaging condition methods (Jin et al., 2014).

The DVB method computes angles from defined vectors. The angle can either be the source and receiver wavefield propagation angle or the incident/reflection angle. There are many definitions for the vectors in the DVB method: the Poynting vector (Dickens and Winbow, 2011), polarization vector, instantaneous-wavenumber (Zhang and McMechan, 2011), energy norm (Rocha et al., 2016) etc. The DVB method is easy to compute and produces high angle resolution, but is not stable for complicated wavefields that contain overlapping events, because of our hypothesis #2.

Let us take the Poynting vector as an example to show how the vectors are computed. The Poynting vector represents the directional energy flux of a wavefield (Stratton, 2007). The Poynting vector computation in seismic wavefield is

$$\mathbf{S} = -\upsilon P = -\nabla P \frac{dP}{dt} P \tag{4}$$

where $\mathbf{S}$ is the Poynting vector, $-\upsilon$ is the velocity vector and P is the stress wavefield (Cerveny, 2005). The $\mathbf{S}$ shares the same direction with the ray trace, so the angle between $\mathbf{S}_{source}$ and $\mathbf{S}_{receivers}$ is twice the value of reflection value.

$$cos2\theta = \frac{\mathbf{S}_{source}\mathbf{S}_{receivers}}{|\mathbf{S}_{source}||\mathbf{S}_{receivers}|} \tag{5}$$

where θ is the reflection angle. so the θ is

$$\theta = \frac{1}{2} arccos \frac{\mathbf{S}_{source}\mathbf{S}_{receivers}}{|\mathbf{S}_{source}||\mathbf{S}_{receivers}|} \tag{6}$$

In 2D, if we set the source stress wavefield as P_s and receiver stress wavefield as P_r, the reflection angle θ turns into

$$\theta = \frac{1}{2} arccos \frac{\frac{dP_s}{dx}\frac{dP_r}{dx} + \frac{dP_s}{dz}\frac{dP_r}{dz}}{\sqrt{(\frac{dP_s}{dx})^2 + (\frac{dP_s}{dz})^2}\sqrt{(\frac{dP_r}{dx})^2 + (\frac{dP_r}{dz})^2}} \tag{7}$$

and vector perpendicular to the reflection plane is

$$\mathbf{S} = (\mathbf{S}_{source} + \mathbf{S}_{receivers})/|cos2\theta| \tag{8}$$

The azimuth can also be computed, and in the 2D case, it is either 0° or 180°. With the angle information, the common angle gather can be obtained after RTM without external computation. To get the ADCIG, the reflection angle θ is introduced in RTM's image condition from equation 5:

$$R(\overrightarrow{x}, \theta) = \int p_B(\overrightarrow{x}, \theta; t) p_F^{-1}(\overrightarrow{x}, \theta; t) dt \tag{9}$$

Amplitude-preserved ADCIGs using subsurface fold

An image point will experience multiple IC values and possibly multiple occurrences of the same reflection angle during the wave propagation process. The quantity of IC values is what we refer to as the "subsurface fold". Then subsurface fold can be a function of space for reflectivity models or a function of space and angle for ADCIGs. Evidently, amplitude increases as subsurface increases for each image point. If the subsurface fold on the reflector layer is not constant, as is usually the case, the amplitudes of the event are not the same and hence erroneous, but its spatial location is correct. When the RTM output is a reflectivity model rather than an ADCIG, the spatial organization and resolution rather than the amplitude control the picture quality. Furthermore, since all IC values are integrated in time at each picture point throughout the IC imaging process, amplitude cannot be exact. We include the subsurface fold into a new IC:

$$R(\overrightarrow{x}, \theta) = f(p_B(\overrightarrow{x}, \theta; t) p_F^{-1}(\overrightarrow{x}, \theta; t)) \tag{10}$$

where $f(x)$ is a weighted function including subsurface fold.

By optimizing the image condition from equation 3 to equation 10, we could state that the output is an amplitude-preserved ADCIGs. However, we can't claim the ADCIGs are true amplitude ADCIGs because, compared with true amplitude common-shot Kirchhoff inversion formula (Keho and Beydoun, 1988), our equation lacks the phase term $i\omega$.

AVA response in Zoeppritz equation, forward modeling, and ADCIG

The Zoeppritz equation can be used to determine the accuracy of AVA response for multi-layer elastic models. However, because theoretical accurate solutions are not available for complicated models we will need to work with simple models to test our ADCIG methodology.

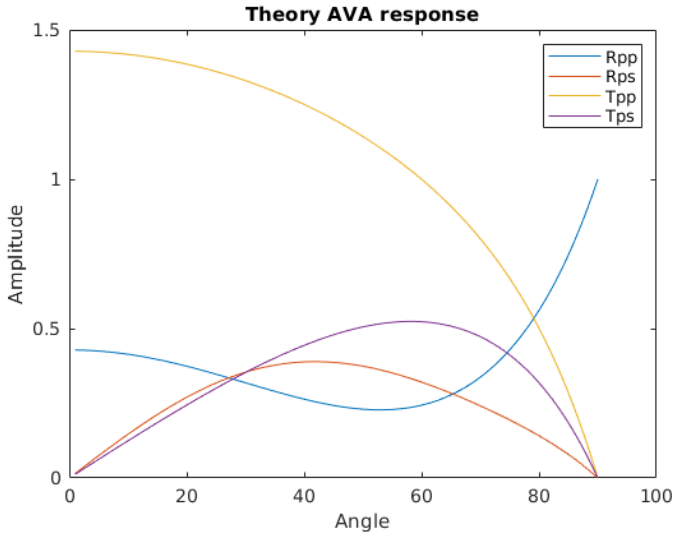

FIG. 3. AVA response from exact Zoeppritz equation

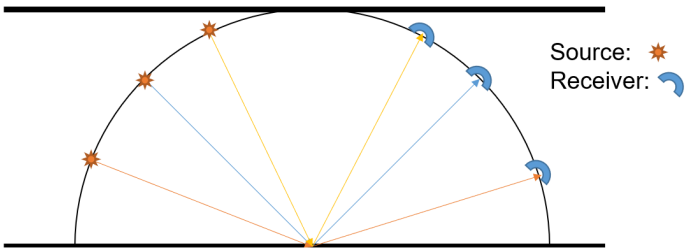

FIG. 4. Coordinates for Finite-difference AVA response

We calculate the gathers for a two-layered elastic model on a grid with 400 cells width and 200 cells depth, and a cell size of 5x5 meters. We set the P/S wave velocity ratio as 0.5, density ratio 0.8, the Poisson's ratio 0.3 and 0.25 for upper and lower layer. The P wave velocity for the first layer is 4000m/s. The theoretical AVA responses calculated from the Zoeppritz equations are shown in Figure 3

Finite-difference forward modelling may also be used to determine the PP wave AVA response, as illustrated in Figure 4. Using the reflector's central image point as a starting point, for each source there is only one active receiver. The incident and reflected ray path lengths are set to a constant to eliminate the changes due to geometrical spreading. Thus, the source is positioned at the top-left corner of the circle, while the receivers are positioned at the top-right corner. Because the incidence angle for the PP wave equals the reflection angles, the source and its matching receiver sites are symmetric. The receiver position for the PS wave may also be calculated using Snell's law.

In the upper two plots of Figure 5, we see the seismic traces and AVA response of the forward modeling for a SH wave in an elastic media with constant density and velocity contrast. In the same Figure but lower two plots, we see the case for constant velocity and density contrast. The direct arrivals are filtered so that only reflected wave remains.

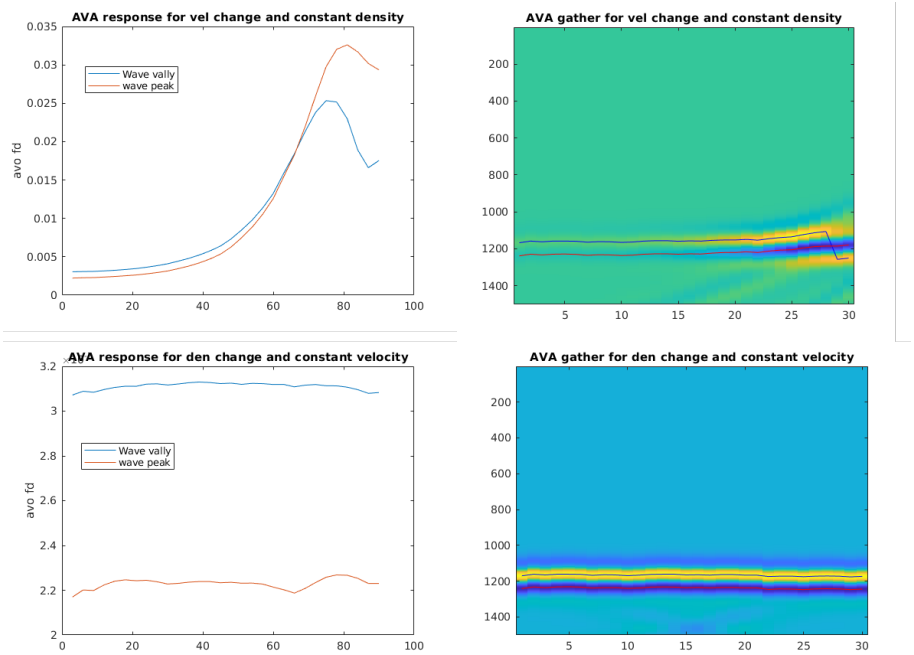

FIG. 5. AVA response curve and seismic trace from 1 velocity change and constant density. 2 density change and constant velocity

The maximum and minimum values are marked on the vertical axes of the seismogram. On the left part of Figure 5 are the AVA responses. It can be seen from the curves that, when the reflector only exist in velocity while the density is constant, the AVA response could indicate the amplitude changes with the reflection angle. But when the reflector only happens in density while velocity is constant, the AVA curve is constant.

In Figure 6 we see the PP wave AVA response of the ADCIGs method for P-SV waves in an elastic media. The blue line is from the Figure 3 and orange line is from ADCIGS. The ADCIGs method for RTM outputs a 4 dimensional data volume: $d(nx, nz, na, nc)$, where nx is the spatial horizontal dimension, nz is the spatial vertical dimension, na is the number of reflection angles (calculated from 0 to 90 degrees), and nc is the value of the subsurface. We pick the image point at the center of the two-layered model.

There is a 1D data set of imaging results with the size of the subsurface offset for each image point and any reflection angle. Using information from the initial velocity as a priori guidance, we eliminated the outliers from the data before selecting a weighted algorithm to obtain a final value signifying the related angle at that image point. A later iteration of the algorithm will likely make it perform better than it does currently. The AVA response curve is smoothed since not all image points fully span the range of reflection angles from 0 to 90 degrees. According to the physical parameter we choose in Figure 3, the majority of the incident energy is reflected as P waves, causing the transmitted P wave and converted S wave to have a modest amplitude and undesirable outcomes. PS wave separation also has a significant impact on the translated S wave accuracy. In order to obtain the amplitude-preserved ADCIGs, we accomplished separation by numerically solving P- and S-wave separated elastic wave equations. However, the results are still unsatisfactory. But it can be seen from Figure 6 that Zoeppritz equations for reflected P wave show similar AVA trends as the responses generated by our ADCIGs method. This gives us some confidence on our

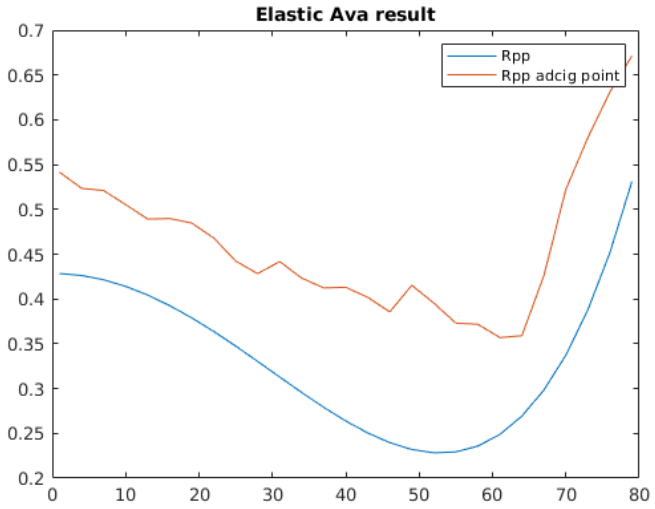

FIG. 6. AVA response from Zoeppritz and ADCIGs for unblended data

methodology of subsurface fold compensation to produce amplitude-preserved ADCIGs.

Blended AVA response

For mixed data, we used the direct migration technique. Figure 7 depicts the horizontal portion of the P wave shot gathers to demonstrate the blended acquisition. Figure 8 displays ADCIGs and Zoeppritz AVA responses for blended data. It is evident that the AVA response from blended data is losing the declining trend at small reflection angles when compared to the AVA response from unblended data. The AVA response from ADCIGs, however, has a general form that resembles that of the Zoeppritz equation. The cross-talk between blended sources is the cause of their differences.

The earlier section demonstrates that our ADCIGs were able to preserve the amplitude of the AVA response. In this part, we demonstrate how direct migration of the blended data might yield outcomes comparable to those of the unblended data, demonstrating that the blended data is still applicable to the ADCIGs extraction technique we employed.

CONCLUSIONS

We defined the term "subsurface fold" in this paper to refer to the fold in subsurface imaging. Then, in order to create ADCIGs, we add it to the RTM image condition. The ADCIGs have been demonstrated to be amplitude-preserved and hence suited for more complicated models after comparing the AVA response with the Zoeppritz equations and simulating forward modelling in a layered model. We can also use our ADCIGs to retrieve data from blended acquisition. The AVA response from blended data processed using the direct migration approach displays attributes similar to those of unblended data, proving that our ADCIG extraction method is fairly effective for blended acquisition.

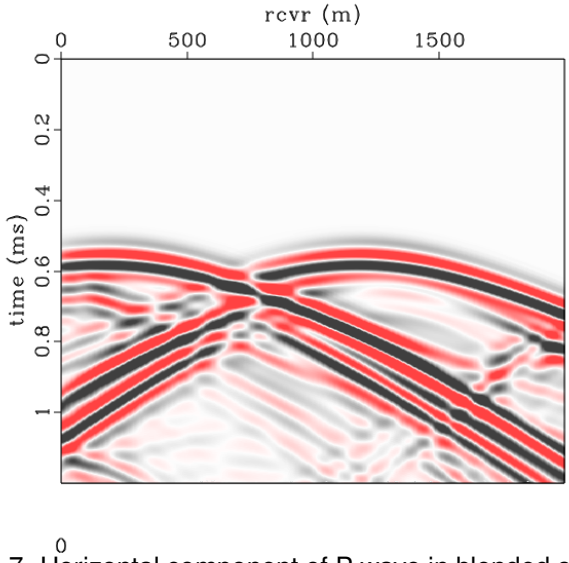

FIG. 7. Horizontal component of P wave in blended shot gather

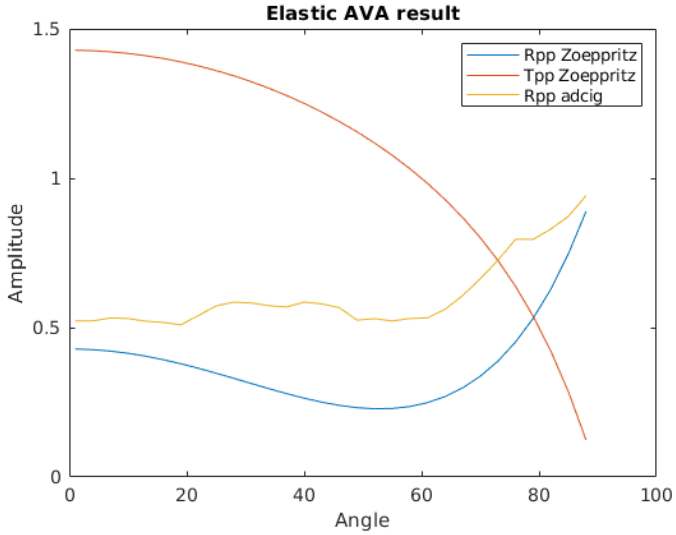

FIG. 8. AVA response from Zoeppritz and ADCIGs for blended data

FUTURE WORK

Least-squares migration

RTM uses an adjoint operator to approximate the inverse of the forward modelling (Claerbout, 1992), which is not a good approximation for the inverse operator. Lailly (1983) introduced the concept of least-squares migration (LSM). Instead of simply using the adjoint migration operator, in LSM the inverse process is sought by attempting to match the data predicted by the model with the observed data. LSM can approximate the inversion operator through either an iterative inversion (Tarantola, 2005; Schuster, 1993; Nemeth et al., 1999) or a single iterative inversion (Rickett, 2003). Moreover, LSM could recover some of the drawbacks of the incomplete seismic data like limited recording aperture, coarse sampling, and acquisition gaps (Nemeth et al., 1999). For blended acquisition, the multi-source LSRTM could suppress migration artifacts in the migration image and remove most of the cross-talk noise from multi-source data (Dai et al., 2010). A possible direction of research for the deblending problem is to apply LSRTM. For OBN data, this should be applied in the common receiver and common angle gathers.

3D applications

Despite the high cost, 3D seismic surveys have many advantages compared with 2D surveys. 3D seismic acquisitions provide a volume of closely spaced seismic data in three dimensions. In contrast, the 2D seismic survey provides a slice of data in two dimensions. Therefore, 3D has a wider field coverage than 2D. Moreover, 3D seismic surveys enhance the signal-to-noise ratio (S/N) significantly (Gaarenstroom, 1984).

In the 2D seismic acquisition, the data is 3D: time, receiver coordinates, and shots coordinates. We could deblend blended shots by transferring data from the shots domain to other domains like the receiver domain, offset domain, and angle domain. The target shot will be coherent, while other shots will be incoherent. However, in a 3D seismic survey, there are five dimensions to represent data in minimum space: inline, crossline, offset, azimuth, and time (other parameterizations are also possible). Deblending through multiple domain transform is difficult because different domains are connected through complex physics. Nevertheless, I believe changing domains will make shots other than shots incoherent since only the target shot has the correct header and time shift.

ACKNOWLEDGMENTS

We thank the sponsors of CREWES for continued support. This work was funded by CREWES industrial sponsors and NSERC (Natural Science and Engineering Research Council of Canada) through the grant CRDPJ 543578-19.

REFERENCES

Abma, R., and Yan, J., 2009, Separating simultaneous sources by inversion, *in* 71st EAGE Conference and Exhibition incorporating SPE EUROPEC 2009, European Association of Geoscientists & Engineers, cp–127.

Akerberg, P., Hampson, G., Rickett, J., Martin, H., and Cole, J., 2008, Simultaneous source separation by

sparse radon transform, *in* SEG Technical Program Expanded Abstracts 2008, Society of Exploration Geophysicists, 2801–2805.

Baysal, E., Kosloff, D. D., and Sherwood, J. W. C., 1983, Reverse time migration: GEOPHYSICS, **48**, No. 11, 1514–1524.

Beasley, C. J., 2008, A new look at marine simultaneous sources: The Leading Edge, **27**, No. 7, 914–917.

Beasley, C. J., Chambers, R. E., and Jiang, Z., 1998, A new look at simultaneous sources, *in* SEG Technical Program Expanded Abstracts 1998, Society of Exploration Geophysicists, 133–135.

Berkhout, A., 2008, Changing the mindset in seismic data acquisition: The Leading Edge, **27**, No. 7, 924–938.

Berkhout, A., Verschuur, D., and Blacquière, G., 2009, Seismic imaging with incoherent wavefields, *in* 2009 SEG Annual Meeting, OnePetro.

Biondi, B., and Shan, G., 2002, Prestack imaging of overturned reflections by reverse time migration, Society of Exploration Geophysicists: SEG Technical Program Expanded Abstracts 2002, 1284–1287.

Bleistein, N., 1987, On the imaging of reflectors in the earth: Geophysics, **52**, No. 7, 931–942.

Bleistein, N., Cohen, J. K., Stockwell Jr, J. W., and Berryman, J., 2001, Mathematics of multidimensional seismic imaging, migration, and inversion. interdisciplinary applied mathematics, vol 13: Appl. Mech. Rev., **54**, No. 5, B94–B96.

Cerveny, V., 2005, Seismic ray theory: Cambridge university press.

Chen, Y., Fomel, S., and Hu, J., 2014, Iterative deblending of simultaneous-source seismic data using seislet-domain shaping regularization: Geophysics, **79**, No. 5, V179–V189.

Claerbout, J. F., 1992, Earth soundings analysis: Processing versus inversion, vol. 6: Blackwell Scientific Publications London.

Dai, W., Boonyasiriwat, C., and Schuster, G. T., 2010, 3d multi-source least-squares reverse time migration, *in* SEG Technical Program Expanded Abstracts 2010, Society of Exploration Geophysicists, 3120–3124.

Dai, W., Wang, X., and Schuster, G. T., 2011, Least-squares migration of multisource data with a deblurring filter: Geophysics, **76**, No. 5, R135–R146.

De Bruin, C., Wapenaar, C., and Berkhout, A., 1990, Angle-dependent reflectivity by means of prestack migration: Geophysics, **55**, No. 9, 1223–1234.

Dickens, T. A., and Winbow, G. A., 2011, Rtm angle gathers using poynting vectors, *in* SEG Technical Program Expanded Abstracts 2011, Society of Exploration Geophysicists, 3109–3113.

Gaarenstroom, L., 1984, The value of 3d seismic in field development: SPE Annual Technical Conference and Exhibition.

Garottu, R., 1983, Simultaneous recording of several vibroseis® seismic lines, Society of Exploration Geophysicists: SEG Technical Program Expanded Abstracts 1983, 308–310.

Jianlei, Z., Zhenping, T., and Chengxiang, W., 2007, P-and s-wave-separated elastic wave-equation numerical modeling using 2d staggered grid, *in* SEG Technical Program Expanded Abstracts 2007, Society of Exploration Geophysicists, 2104–2109.

Jin, H., McMechan, G. A., and Guan, H., 2014, Comparison of methods for extracting adcigs from rtm: Geophysics, **79**, No. 3, S89–S103.

Keho, T., and Beydoun, W., 1988, Paraxial ray kirchhoff migration: Geophysics, **53**, No. 12, 1540–1546.

Lailly, P., Bednar, J. et al., 1983, Conference on inverse scattering: Theory and application: The seismic inverse problem as a sequence of before stack migration, 206–220.

Leader, C., and Biondi, B., ????, Image space separation of linearly blended data.

Mahdad, A., Doulgeris, P., and Blacquiere, G., 2011, Separation of blended data by iterative estimation and subtraction of blending interference noise: Geophysics, **76**, No. 3, Q9–Q17.

McMECHAN, G. A., 1983, Migration by extrapolation of time-dependent boundary values*: Geophysical Prospecting, **31**, No. 3, 413–420.

Moore, I., Dragoset, B., Ommundsen, T., Wilson, D., Ward, C., and Eke, D., 2008, Simultaneous source separation using dithered sources, *in* SEG Technical Program Expanded Abstracts 2008, Society of Exploration Geophysicists, 2806–2810.

Nemeth, T., Wu, C., and Schuster, G. T., 1999, Least-squares migration of incomplete reflection data: Geophysics, **64**, No. 1, 208–221.

Nolan, C. J., and Symes, W. W., 1996, Imaging and coherency in complex structures.

Ostrander, W., 1984, Plane-wave reflection coefficients for gas sands at nonnormal angles of incidence: Geophysics, **49**, No. 10, 1637–1648.

Ren, Z., and Li, Z. C., 2017, Temporal high-order staggered-grid finite-difference schemes for elastic wave propagationtemporal high-order sfd schemes: Geophysics, **82**, No. 5, T207–T224.

Rickett, J. E., 2003, Illumination-based normalization for wave-equation depth migration: Geophysics, **68**, No. 4, 1371–1379.

Rickett, J. E., and Sava, P. C., 2002, Offset and angle-domain common image-point gathers for shot-profile migration: Geophysics, **67**, No. 3, 883–889.

Rocha, D., Tanushev, N., and Sava, P., 2016, Isotropic elastic wavefield imaging using the energy norm: Geophysics, **81**, S207–S219, http://dx.doi.org/10.1190/geo2015-0487.1.
URL http://dx.doi.org/10.1190/geo2015-0487.1

Sava, P. C., and Fomel, S., 2003, Angle-domain common-image gathers by wavefield continuation methods: Geophysics, **68**, No. 3, 1065–1074.

Schuster, G. T., 1993, Least-squares cross-well migration, *in* SEG Technical Program Expanded Abstracts 1993, Society of Exploration Geophysicists, 110–113.

Stratton, J. A., 2007, Electromagnetic theory, vol. 33: John Wiley & Sons.

Tang, Y., and Biondi, B., 2009, Least-squares migration/inversion of blended data, *in* SEG Technical Program Expanded Abstracts 2009, Society of Exploration Geophysicists, 2859–2863.

Tarantola, A., 2005, Inverse problem theory and methods for model parameter estimation: SIAM.

Vyas, M., Nichols, D., and Mobley, E., 2011, Efficient rtm angle gathers using source directions, *in* 2011 SEG Annual Meeting, OnePetro.

Whitmore, N. D., 2005, Iterative depth migration by backward time propagation: SEG Technical Program Expanded Abstracts 1983, 382–385, https://library.seg.org/doi/pdf/10.1190/1.1893867.
URL https://library.seg.org/doi/abs/10.1190/1.1893867

Xu, S., Chauris, H., Lambaré, G., and Noble, M., 2001, Common-angle migration: A strategy for imaging complex media: Geophysics, **66**, No. 6, 1877–1894.

Zhang, Q., and McMechan, G. A., 2011, Common-image gathers in the incident phase-angle domain from reverse time migration in 2d elastic vti media: Geophysics, **76**, No. 6, S197–S206.

Zhang, Y., and Sun, J., 2009, Practical issues in reverse time migration: True amplitude gathers, noise removal and harmonic source encoding: First break, **27**, No. 1.

Zhang, Y., Zhang, G., and Bleistein, N., 2005, Theory of true-amplitude one-way wave equations and true-amplitude common-shot migration: Geophysics, **70**, No. 4, E1–E10.